MODELING THE REBOUNDING OF CONTAMINANT CONCENTRATIONS IN SUBSURFACE GASEOUS PHASE DURING INTERMITTENT SOIL VAPOR EXTRACTION OPERATION

Mei-Sheue Wang,[1,2] Shian-Chee Wu[1,*] and Chun-Wei Kuo[1]

[1]Graduate Institute of Environmental Engineering
National Taiwan University
Taipei 106, Taiwan
[2]Department of Environmental Engineering,
Vanung University
Taoyaun 320, Taiwan

Key Words: Rebounding, soil vapor extraction, volatile organic compound, mass transfer, stagnant region

ABSTRACT

Soil vapor extraction (SVE) process for contaminated soil remediation often shows a tailing of the breakthrough concentration in the contaminant plume and rebounding of gaseous phase concentration after a pause of the extraction operation. These phenomena are believed to have something to do with the limitation of mass transfer between mobile fluid and some stagnant aggregates or clay lens. An advection-diffusion mass transport model in unsaturated soil with the consideration of diffusive mass transfer between the mobile regions and the immobile regions was adopted to simulate the rebounding of gaseous phase concentrations of some volatile organic compounds (VOCs). Experimental results of a pilot scale SVE showed that after being lowered to one-tenth of the initial concentration levels, concentrations of VOCs in the monitoring well rebounded significantly up to about 20% of the initial concentrations again. Model simulation could explain the rebounding phenomenon and fit the data well by only adjusting the volume fraction of the immobile regions, the averaged radius of the aggregates and the standard deviation of the logarithmic mass transfer coefficient. The model will be able to assist the designing of the SVE system and operational strategy, and the prediction of the performance of the clean-up action.

INTRODUCTION

In-situ soil vapor extraction (SVE) is one of the common approaches for the remediation of vadose zone of soils contaminated by volatile organic compounds. Although SVE has been shown to be effective in reducing pollutant contents in soil, there are limitations to its use. The SVE process often shows an initially fast pace of removing contaminants followed by an extremely slow pace. The tailing phenomenon of the breakthrough of contaminant plume results in a clean-up time ten to a hundred times longer than the fluid contact time [1-3]. Also, with SVE approach being used, the concentrations of the organic contaminants in the soil gas are reduced rapidly to a very low level in a short period of time; however, after a brief pause in the extraction operation, the contaminant concentrations in the soil gas rise sharply to reach a new plateau. This phenomenon has been named the "rebounding" effect [4-5].

For physically adsorbed organic compounds, the rates of adsorption or desorption with mineral surfaces (or organic films on mineral grains) are usually fast, and the system could reach equilibrium as quickly as in a few min or up to a few h [6-9]. Thus, the tailing and rebounding phenomena must have something to do with the slow fluid movement in certain mass-transfer-limiting regions in soils. Inside the stagnant areas there is a very low flow of fluid due to the fine texture of the soil matrix (like fine clay particles) or an existence of aggregates containing a denser fluid (e.g., water) relative to that (e.g., air) in the bulk region (the dark areas in Fig. 1). The solutes cannot be easily removed from the area for there is no fluid advection in the stagnant region.

In order to describe the phenomenon of tailing and rebounding of a pollutant breakthrough curve, researchers have modeled the pollutant transport in
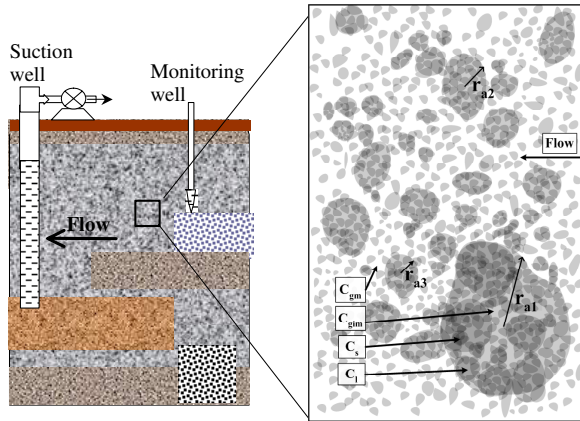
*Corresponding author
Email: scwu@ntu.edu.tw

Fig.1. A heterogeneous soil zone contains many stagnant regions (the dark areas) in which the advection is insignificant due to a low hydraulic conductivity and the mass transfer occurs only by diffusion.

groundwater by a two-region model which divides the soil matrix into two regions (sites), in one of which the transport is controlled by advection and in another the transport is controlled by pollutant mass transfer. Researchers also described the rate of uptake and release of an organic compound in and out of an immobile region by a first-order mass transfer model; that is, the rate of concentration change is proportional to the difference of the concentrations:

$$\text{rate} = \alpha \, (C_{gm} - C_{gim}) \tag{1}$$

where α is the first-order mass transfer coefficient (h^{-1}), C_{gm} is the gaseous concentration in the mobile region ($mg \, cm^{-3}$) and C_{gim} is the gaseous concentration in the adjacent immobile region ($mg \, cm^{-3}$) [4, 10-19].

Although the two-region model is simple, this model could not explain the phenomenon of tailing with a single uniform transfer coefficient. Culver et al. [20] and Deitsch et al. [21] have instead separated soil stagnant regions into many classes, with each class being assigned a specific mass-transfer coefficient. Model simulation with these transfer coefficient sets in a log-normal distribution or in a gamma (Γ) distribution could be fitted to the experimental results well by adjusting only two characterizing parameters, the mean and the deviation. Wang et al. [22] have been using a set of log-normal distributed mass transfer coefficients in the transport model to describe the tailing breakthrough curves in laboratory soil columns and on a field SVE site. In order to independently estimate the distribution of the values of the transfer coefficients, Wang et al. have correlated the coefficients to the soil properties and the site characteristics. They found that the value of the best-fitting transfer coefficient was inversely correlated with the dimension of the site.

For the sorption of organic compounds by suspended sediment aggregates Wu and Gschwend [23]

have established a relationship among the α, the effective intra-aggregate diffusivity, D_{eff}, and the aggregate radius, r_a,

$$\alpha = 22.7 \, D_{eff} \, r_a^{-2} \tag{2}$$

where D_{eff} is given by

$$D_{eff} = \frac{D_l \theta}{\theta + \rho K_s} \tag{3}$$

in which D_l is the molecular diffusivity ($cm^2 \, s^{-1}$), θ is the liquid content ($cm^3 \, cm^{-3}$), ρ is the bulk solid density ($g \, cm^{-3}$), K_s is the solid-water distribution coefficient ($cm^3 \, g^{-1}$) and r_a is the radius of the aggregate (cm).

Information on the size distribution of immobile regions has so far been rarely reported. However, it has been shown in the literature that the aggregate sizes, expressed in log scale, generally follow a normal distribution pattern [24-26], which has been used to estimate the distribution of the respective mass-transfer coefficients associated with the immobile regions [27-28].

Since the rebounding of contaminant concentrations in monitoring wells during SVE remediation operation is a frequently-observed problem, the capability to predict its behavior is essential while choosing an appropriate remediation approach or operational procedures. In this study we intended to explain the rebounding phenomenon observed in a pilot scale experimental site by using this dual-region (mobile/immobile) transport model, which contains a set of mass-transfer coefficients to quantify the sorption and desorption rates between the mobile and immobile regions. Also, simulations on different operation conditions were performed to illustrate the capability of this model to predict the efficiency of different SVE operational approaches.

MATERIALS AND METHODS

1. Field Experiments and Sampling Methods

The field test of SVE remediation method was conducted in the experimental farm of National Taiwan University in Shindian, a suburban of Taipei city. The geological setting of the site includes grayish dark silty loam with sands within the top 0.5 m of the unsaturated zone, yellow brown sandy loam between 0.5 and 1.5 m, silt with some clay lens between 1.5 and 4.5 m, and a layer of clay beneath the depth of 4.5 m. The organic carbon fraction is 0.44% (w/dry w) measured with the dichromate oxidation method [29].

The SVE site had a radius of 300 cm and was laid with 15 cm of bentonite on the ground surface to prevent air leaking into the suction well (Fig. 2). The suction well had a diameter of 15.24 cm. It was connected to a demister and a vacuum pump. The screen opened between 1 m and 4 m below ground surface with a total opening length of 3 m.
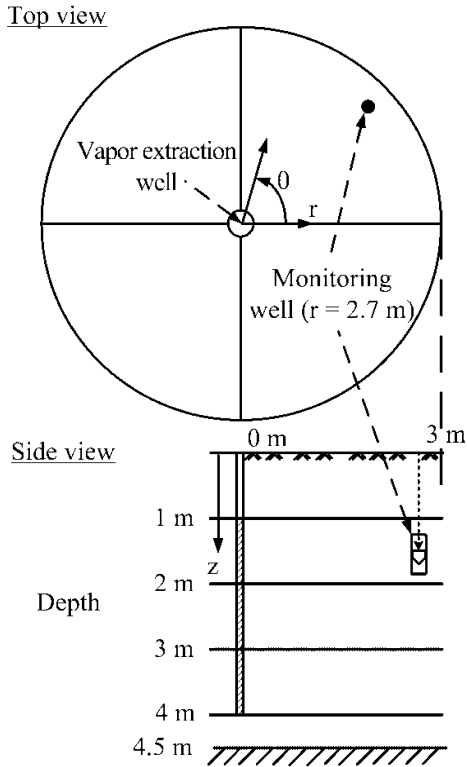
Fig. 2. Layout of the soil vapor extraction field test site and the location of the suction well and the monitoring well.

Approximately equal volumes of n-hexane, cyclohexane, isooctane, n-heptane, ethylbenzene, and xylene (containing *m*-xylene, *p*-xylene and *o*-xylene) were mixed and used as testing compounds. The properties of these seven organic compounds are list in Table 1. The mixture of compounds was injected into the unsaturated zone between 1.0 and 1.5 m through 19 evenly distributed injection wells in a quarter of a circle surrounding the suction well. Suction, actually a part of a bioventing operation, had started and operated intermittently for one yr before the rebounding experiment started.

The SVE system had been shut off for two wk right before the rebounding experiments to allow the concentrations of compounds in soil to reach equilibrium among phases. Then, samples were taken with a hand pump from monitoring well located 270 cm away from the suction well, with the opening at the depth of 1.5 m below ground surface. The monitoring well was installed in a 5.08 cm hole by applying a direct-push-in probe. A Teflon tube was put in with a screened aluminum head at the desired positions, then the surrounding of the head was stuffed with quartz sands and lastly the hole was sealed with bentonite.

Samples were analyzed with a gas chromatograph equipped with a flame ionization detector (Hewlett Packer, HP 5890) for the gaseous concentrations of compounds before and after the experiments

started. The concentrations measured right before the suction process were served as the initial conditions of model simulation for concentration variations.

2. Model Development

Since the layout of the SVE system, including the distribution of the spiked compound concentration, is symmetrical to the suction well, a cylindrical coordinate system was adopted while constructing the transport model. Equation 1 is adopted to describe the rate of concentration change in the immobile regions. For a number of immobile regions in a heterogeneous soil matrix, the distribution of the fractions of immobile regions, based α, associated with these regions, may be described by a certain distribution function. Following this approach, we define the distribution of the total fraction of the immobile regions with mass-transfer coefficients lower than α as a log-normal distribution function. Let us transform the coordinate into logarithmic scale and define y as

$$ y = \log(\alpha) \qquad (4) $$

Then, by assuming the probability density of the volume fraction of an immobile region with respect to y to be a normal distribution, $f(y)$, one gets

$$ f(y) = \frac{1}{\sqrt{2\pi}\sigma} \exp\left(\frac{-(y-\mu)^2}{2\sigma^2} \right), $$
$$ -\infty < y < \infty \qquad (5) $$

where μ is the average of $\log(\alpha)$, σ is the standard deviation of $\log(\alpha)$ [30]. Adopting a numerical approach, we divide immobile regions into N groups, with coefficient α_j and fraction (probability intensity) f_{sj} for the jth group, and

$$ \sum_{j=1}^{N} f_{sj} = 1 \qquad (6) $$

The total concentration of the organic compound, C_T, in a space containing solid, liquid and gaseous phases, is as follows:

$$ C_T = aC_g + \theta C_l + \rho C_s $$
$$ = F_m aC_{gm} + (1-F_m)aC_{gim} + \theta C_l + \rho C_s \qquad (7) $$

where C_g is the concentration in the gaseous phase (mg cm^{-3}), C_l is the concentration in the liquid phase (mg cm^{-3}), C_s is the concentration in the solid phase (mg g^{-1}), a is the gas content (cm^3 cm^{-3}). The concentration in the gaseous phase, C_g, is the weighted average of the concentration in the air phase of the mobile regions, C_{gm}, and that in the immobile regions, C_{gim}. F_m is the volume fraction of the mobile regions (cm^3 cm^{-3}) where the advection of the tracer in the air phase dominates the transport.

Because the liquid in a vadose zone always adheres on the surfaces of soil pellets, the contaminants in solid and liquid phases are stationary. Hence, the

Table 1. The properties of the organic chemicals

	$D_l{}^a$	$D_f{}^b$	$K_h{}^c$	Log $(K_{ow})^d$	$K_d{}^e$	R^f	α^g
n-hexane	8.73	0.0765	56.49	3.9	0.2537	0.57	0.0079
cyclohexane	9.89	0.0840	7.28	3.44	0.6828	1.30	0.025
isooctane	7.41	0.0655	93.46	5.02	2.0212	3.48	0.00051
n-heptane	8.00	0.0704	81.65	4.66	1.0099	1.82	0.00128
ethylbenzene	8.54	0.0735	0.32	3.15	7.8391	13.60	0.0396
m,p-xylene	8.54	0.0735	0.19	3.16	13.7241	23.69	0.0396
o-xylene	8.54	0.0735	0.19	3.16	13.7241	23.69	0.0396

[a]The molecular diffusion coefficients of compounds in water (D_l, 10^{-6} cm^2 s^{-1}) were estimated by using Hayduk and Laudie method, in Schwarzenbach et al. [34].

[b]The molecular diffusion coefficients of compounds in air (D_f, cm^2 s^{-1}) were estimated by using Fuller's method, in Schwarzenbach et al. [34].

[c]Henry's law constant (K_h, M M^{-1}).

[d]Octanol-water partition coefficient (K_{ow}).

[e]Solid-gas partition coefficient (K_d, (mg L^{-1}) (mg L^{-1})$^{-1}$). The K_d of tracer is estimated by using: $K_d = \dfrac{f_{oc} \cdot K_{oc}}{K_h} =$

$\dfrac{f_{oc} \cdot (0.41 K_{ow})}{K_h}, f_{oc} = 0.44\%$ (w/dry w).

[f]Retardation factor (R).

[g]Mass transfer coefficient (α, h^{-1}).

liquid and solid phases are grouped into immobile regions. In a length as small as a mineral grain, the concentrations of an organic compound in liquid and solid phases can be assumed to be in equilibrium locally. With the assumption of that C_{gim} is in equilibrium with the concentrations in liquid and solid phases, one obtains, at low tracer concentrations with moist soils [31], the relations of

$$C_s = K_d C_{gim} \qquad (8)$$

and

$$C_l = \frac{C_{gim}}{K_h} \qquad (9)$$

where K_d is the compound partition coefficient between the solid and gas phases; K_h is the partition coefficient between the gas and liquid phases (i.e. Henry's law constant). Substituting Eqs. 8 and 9 into Eq. 7, one arrives at

$$C_T = F_m a C_{gm} + (1-F_m) a C_{gim} + \frac{\theta}{K_h} C_{gim}$$

$$+ \rho K_d C_{gim} = F_m a C_{gm} + R C_{gim} \qquad (10)$$

$$R = (1-F_m) a + \frac{\theta}{K_h} + \rho K_d \qquad (11)$$

By averaging the whole cross-sectional area, the total concentration, C_T, is

$$C_T = F_m a C_{gm} + R \sum_{j=1}^{N} (f_{sj} C_{gim,j}) ; j = 1,2,\cdots N \qquad (12)$$

The mass fluxes of contaminants are attributed mainly to the advection in the gaseous flow. For an one-dimensional, incompressible uniform flow due to

the concentration gradients in an isotropic soil layer with negligible density effects, the change of the cross-sectional, averaged contaminant concentration can be described by using the advection-dispersion equation [32]. In addition, with the radial flow dominating the transport of compounds, the vertical and lateral transport of mass was neglected. The density of air in the soil was assumed constant since the maximum pressure drop in the monitoring wells in the SVE site was only 4 kPa. The governing equation of the transport of a compound in a cylindrical coordinate system can be expressed as [33]

$$\frac{\partial C_T}{\partial t} = F_m a D_g \left[\frac{\partial^2 C_{gm}}{\partial r^2} + \frac{1}{r} \frac{\partial C_{gm}}{\partial r} \right]$$

$$- F_m a \frac{\partial (U_g C_{gm})}{\partial r} \qquad (13)$$

$$D_g = D_f + D_m \qquad (14)$$

$$D_m = \alpha_L U_g \qquad (15)$$

$$U_g = \frac{Q}{(2\pi r H) F_m a} \qquad (16)$$

where D_g is the dispersion coefficient of the gas flow in the mobile phase, D_f is the molecular diffusion coefficient (cm^2 h^{-1}) in air, D_m is the mechanical dispersion coefficient (cm^2 h^{-1}), α_L is dispersivity (cm), U_g is the average linear flow velocity of the gas flow in the mobile regions (cm h^{-1}), Q is the total flow rate (cm^3 h^{-1}), H is the thickness of the contaminated soil

layer (cm) (i.e., the length of the screen opening), and r is the radial dimension (cm).

Then, by substituting Eq. 12 into Eq. 13, the governing transport equation can be expressed as

$$F_{\mathrm{m}}a\frac{\partial C_{\mathrm{gm}}}{\partial t} + R\sum_{j=1}^{N}(f_{sj}\frac{\partial C_{gim,j}}{\partial t})$$

$$= F_{\mathrm{m}}aD_{\mathrm{g}}\left[\frac{\partial^2 C_{\mathrm{gm}}}{\partial r^2} + \frac{1}{r}\frac{\partial C_{\mathrm{gm}}}{\partial r}\right]$$

$$- F_{\mathrm{m}}a\frac{\partial(U_{g}C_{gm})}{\partial r}; \; j=1,2,\cdots N \qquad (17)$$

For the jth group of the immobile regions, the total change in concentration with time ($\partial C_{gim,j}/\partial t$) is equal to the product of the mass transfer coefficient and the difference of gasous concentrations inside and outside the region, i.e.,

$$\frac{\partial C_{gim,j}}{\partial t} = [\alpha_j(C_{gm} - C_{gim,j})]; \; j=1,2,\cdots N \quad (18)$$

That is,

$$R\sum_{j=1}^{N}(f_{sj}\frac{\partial C_{gim,j}}{\partial t}) = R\sum_{j=1}^{N}\left[f_{sj}\alpha_j(C_{gm} - C_{gim,j})\right];$$

$$j=1,2,\cdots N \qquad (19)$$

in which α_j is the mass-transfer coefficient of the jth immobile region. Thus, the governing transport equation is finally cast as follows:

$$\frac{\partial C_{\mathrm{gm}}}{\partial t} = D_{\mathrm{g}}\frac{\partial^2 C_{\mathrm{gm}}}{\partial r^2} + \frac{D_{\mathrm{g}}}{r}\frac{\partial C_{\mathrm{gm}}}{\partial r} - \frac{\partial(U_{g}C_{gm})}{\partial r}$$

$$- \frac{R\sum_{j=1}^{N}\left(f_{sj}\alpha_j(C_{gm} - C_{gim,j})\right)}{F_{\mathrm{m}}a}; \; j=1,2,\cdots N \quad (20)$$

In the above equation, the dispersivity values, partition coefficient and mass-transfer coefficients were calibrated by using real data. All other parameters were measured on site. The air-extracting flow rate, Q, is $3.63 \times 10^7 \, \mathrm{m^3\,h^{-1}}$.

A finite-difference numerical scheme written in Fortran program language was used to solve Eq. 20 for the concentration of the compound in the gas phase at different times and locations in the SVE system.

The boundary conditions and the initial condition are

$$C_{gm} = 0, \text{ at } r = \infty \qquad (21)$$

C_{gm} = measured values, at

$$r \le 280 \, \mathrm{cm}, t = 0 \qquad (22)$$

$$\frac{\partial C_{gm}}{\partial r} = 0, \text{ at } r = 7.12 \, \mathrm{cm}$$

$$\text{(the radius of the suction well)} \qquad (23)$$

3. Model Calibration

Model calibration was conducted by adjusting the values of the average of log α, μ, and the standard deviation of log α, σ, until a minimum deviation (sum of square errors) was obtained between the solution of Eq. 20 and the real measurements. By assuming that the immobile regions are approximately spherical, we may relate the transfer coefficient to the effective diffusivity, D_{eff}, and the radius of the immobile region, r_a, with the following equation [23]:

$$r_a = 4.73 D_{\mathrm{eff}}^{0.5}\alpha^{-0.5} \qquad (24)$$

where r_a is the radius of the immobile region, and D_{eff} is the effective diffusion coefficient.

Since the D_{eff} can be estimated based on the known properties of the organic compounds of concern and the soil properties of the soil on the site, the parameter that we have to adjust in the model is the radius of the immobile regions.

RESULTS AND DISCUSSION

1. SVE Field Experiments

The concentrations of seven organic compounds in the gaseous phase of the monitoring well were taken at different times, as data shown in Fig. 3. During the period of vapor extraction, the concentrations in the gaseous phases all dropped below few percents of the initial concentrations in 20 h. However, significant rebounding of the concentration in the gaseous phase was observed after halting the extraction. The gaseous concentration of VOCs was gradually raised to 15 to 20% of the initial concentration for each compound. The operation of extraction removed most of the compounds in the gas phases in mobile regions rapidly though it might only have removed part of the compounds in the immobile regions. The compounds retained in the stagnant regions escaped slowly from the stagnant regions by diffusion and resulted in rebounding of concentrations in the gaseous phases. Towards the end of the observation, 60 h after halting the extraction, the concentrations of the gaseous phase were still climbing and had not reached stable plateaus yet.

2. Model Simulation

Model simulations were performed to help explain the variation of the compound concentration during the intermittent SVE operation. The system parameters are listed in Tables 1 and 2.

The results of model simulations are shown in Fig. 3. A universal average and its standard deviation of the radii of the immobile regions were used for all compounds. The best fitting parameters are shown in Table 2. The best-fitting averaged radius of the immo-
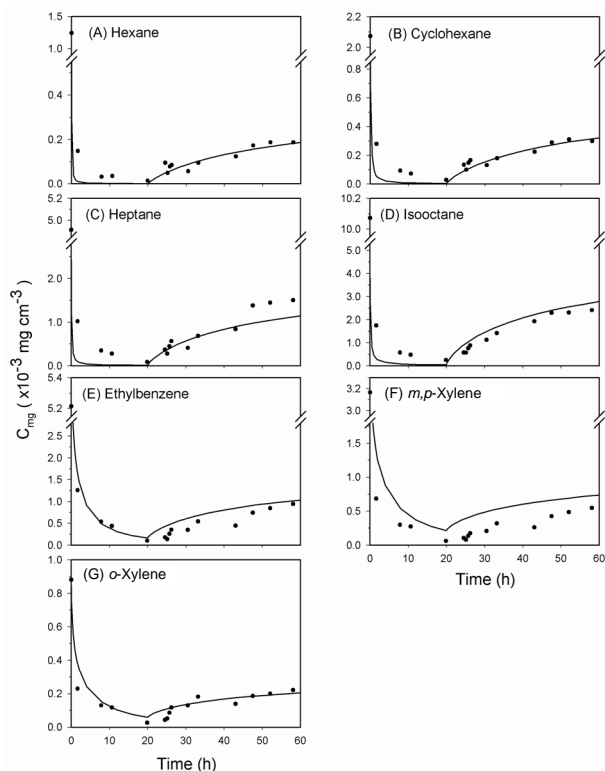
Fig. 3. Concentrations of seven organic compounds in the gaseous phase at the monitoring well in the SVE field test site (solid circles) and the best-fitting model simulation results (solid line).

Table 2. The modeling parameters and the results of model calibration

Model parameters	Values
Width (cm)	60
Dispersivity (cm), α_L (fitted)	18.9
Total porosity	0.416^a
Water content, θ	0.171^a
Gas volume fraction, a	0.245^a
Air-extracting flow rate (cm^3 h^{-1})	3.63×10^7
Simulation results and the best fitting values	
F_m (fitted)	0.4
Averaged radius of the aggregate (cm), r_a (fitted)	0.8
Mass transfer coefficient	
Average α ($\times 10^{-4}$ h^{-1}) (calculated)	$5.1\sim39.6^b$
Standard deviation of log α (h^{-1}) (fitted)	2.1

^{a} The average values.
^{b} The average mass transfer coefficient is calculated by Eq. 2.
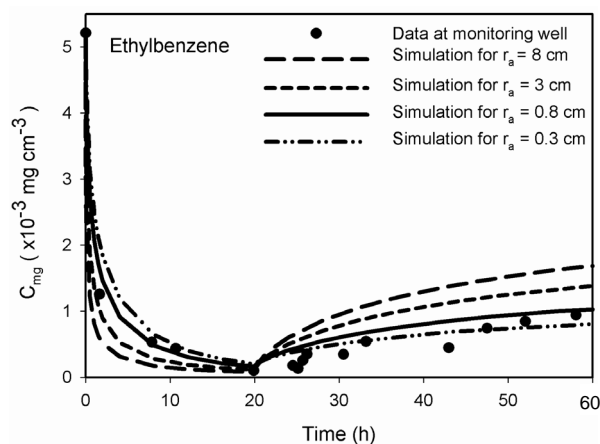

Fig. 4. The sensitivity analyses for the length scale of the stagnant aggregates in the SVE field test site.

bile regions is 0.8 cm and the standard deviation of the log-normal distribution of mass transfer coefficients is 2.1 (log scale). Comparing the different compounds, we found that the model overestimates the removal rates during extraction for hexane, cyclohexane, heptane and isooctane; however, simulation fits the data for ethylbenzene, *m,p*-xylene and *o*-xylene. After halting the extraction, the model slightly overestimates the recovery of ethylbene, and *m,p*-xylene. All estimations are generally within 76 to 135% of the observed values at the end of the experiment.

The simulation results reflect the effects of higher Henry's law constants and lower partition coefficients of hexane, cyclohexane, heptane and isooctane on higher releasing tendency (concentration gradient between the inside and the out side of the immobile regions) during the suction period. The experimental results did not follow the same trend. The reason of this discrepancy will be the topic of our future research.

Sensitivity analyses of the averaged radius of the immobile regions shows that with larger radius of the stagnant regions (e.g., 8 cm), the ethylbenzene concentration drops faster during the suction period and rebounds higher at 60 h after halting the suction (Fig. 4). The reason of the rapid drop is that the larger stagnant regions possess larger storage capacity and longer diffusive paths; therefore, the compounds in

the mobile regions are rapidly exhausted. This also creates a false cleaned-up observation when SVE is applied in the field. However, during the rebounding period, higher amount of compounds preserved in the stagnant regions serve as stronger and more lasting sources and result in more vigorous rebounding.

The results of the simulation also indicate that the best-fitting radii of the immobile regions are independent of the type of the compounds. The dimensions of the immobile regions are properties of the soil and the SVE site.

Simulation result shows that for ethylbenzene, as an example, 97% of ethylbenzene in the mobile regions was removed after 20 h however, only 46% of ethylbenzene in the immobile regions was removed (Fig. 5). 40 h after the suspension of the extraction, simulation and field experiment coincidently show that ethylbenzene escaped from the immobile regions, entered the gaseous phase and raised the concentration to 20% of the original concentrations, though, the con-
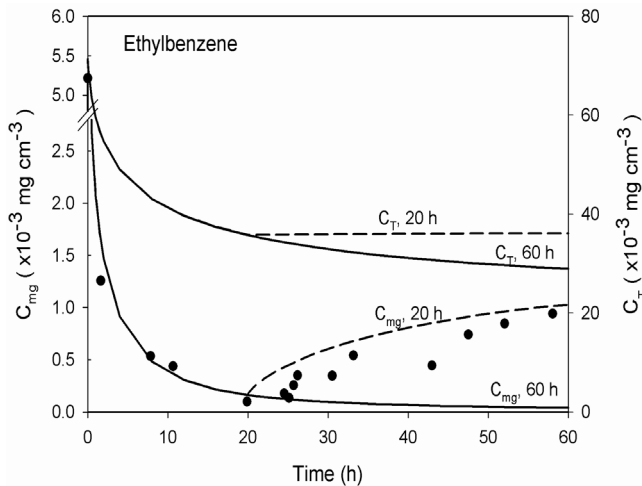
Fig. 5. Concentrations of ethylbenzene in the gaseous phase at the monitoring well in the SVE field test site (solid circles). Solid lines indicate the best-fit model simulation results total concentration and gaseous concentration, for continuous suction in the SVE field test site. Segmented lines indicate the model simulation results for the total concentration and gaseous concentration if suction were stopped at the 20 h and there were only diffusion between mobile and immobile regions till 60 h.

tent in the immobile regions has no observable change for 40 h.

CONCLUSIONS

Experimental results did show the concentration rebounding phenomenon during the intermittent SVE operation. The gaseous concentration of VOCs dropped to less than 4% of the initial concentrations; however, it was gradually raised to 15 to 20% of the initial concentration for each compound. The dual-region, mass-transfer limiting transport model developed in this study not only explains the phenomenon of rebounding well but it can also be used to predict the time required to clean up a contaminated site by soil vapor extraction. The only fitting parameters are the volume fraction of the immobile regions, the averaged radius of the aggregates and the standard deviation of the logarithmic mass transfer coefficient. The model will be able to assist in the designing of the SVE system and operational strategy, and the prediction of the performance of the clean-up action. Further researches should be directed to the emphases on characterizing, measuring or predicting the size distribution of the aggregates, relating the fraction of the immobile regions to the physical properties and hydrological conditions of the soil layer, and chemical properties on the mass transfer rate.

NOMENCLATURE

C_g	Concentration in the gaseous phase, mg cm^{-3}
C_{gm}	Gaseous concentration in the mobile region, mg cm^{-3}
C_{gim}	Gaseous concentration in the immobile region, mg cm^{-3}
C_l	Goncentration in the liquid phase, mg cm^{-3}
C_s	Concentration in the solid phase, mg g^{-1}
C_T	Total concentration of the organic compound, mg cm^{-3}
D_{eff}	Effective diffusion coefficient of the tracer in the aggregates, cm^2 h^{-1}
D_f	Molecular diffusion coefficient in air, cm^2 h^{-1}
D_g	Dispersion coefficient of the gas flow in the mobile phase, cm^2 h^{-1}
D_l	Molecular diffusivity of the compound in water, cm^2 h^{-1}
D_m	Mechanical dispersion coefficient, cm^2 h^{-1}
F_m	Volume fraction of the mobile regions, cm^3 cm^{-3}
H	Thickness of the contaminated soil layer, cm
K_d	Tracer partition coefficient between the solid and gas phases, (mg L^{-1})(mg L^{-1})$^{-1}$
K_h	Henry's law constant, M M^{-1}
K_s	Solid-water distribution coefficient
K_{ow}	Octanol-water partition coefficient
Q	Total flow rate, cm^3 h^{-1}
R	Retardation factor
U_g	Average linear flow velocity of the gas flow in the mobile regions, cm h^{-1}
a	Gas volume fraction, cm^3 cm^{-3}
f_{sj}	Fraction of the jth group
r	Radial dimension, cm
r_a	Averaged radius of the aggregate, cm
α	First-order mass transfer coefficient, h^{-1}
α_j	Mass-transfer coefficient of the jth immobile region, h^{-1}
α_L	Dispersivity, cm
μ	Average of log α, h^{-1}
θ	Liquid content, cm^3 cm^{-3}
ρ	Bulk density, g cm^{-3}
σ	Standard deviation of log α

REFERENCES

1. Griffioen, J., Suitability of the first-order mass

transfer concept for describing cyclic diffusive mass transfer in stagnant zones. J. Contam. Hydrol., 34(1-2), 155-165 (1998).

2. Lorden, S.W., W. Chen and L.W. Lion, Experiments and modeling of the transport of trichloroethene vapor in unsaturated aquifer material. Environ. Sci. Technol., 32(13), 2009-2017 (1998).

3. Miller, C.T., G. Christakos, P.T. Imhoff, J.F. McBride and J.A. Pedit, Multiphase flow and transport modeling in heterogeneous porous media: challenges and approaches. Adv. Water Resour., 21(2), 77-120 (1998).

4. Nelson, N.T., Q. Hu and M.L. Brusseau, Characterizing the contribution of diffusive mass transfer to solute transport in sedimentary aquifer systems at laboratory and field scales. J. Hydrol., 276(1-4), 275-286 (2003).

5. Wilson, J. and L.J. Lin, Dueling time constants: competing processes in aquifer contamination and remediation. Proceedings, International Conference on Groundwater Quality Protection – Remedial Technology and Management Policy for NAPL Contamination. Taipei, Taiwan, pp. 269-303 (1997).

6. Chang, M.L., S.C. Wu and C.Y. Chen, Diffusion of volatile organic compounds in pressed humic acid disks. Environ. Sci. Technol., 31(8), 2307-2312 (1997).

7. Chang, M.L., S.C. Wu, P.J. Chen and S.C. Cheng, Infrared investigation of the sequestration of toluene vapor on clay minerals. Environ. Toxicol. Chem., 22(9), 1956-1962 (2003).

8. Shih, Y.H. and S.C. Wu, Sorption kinetics of toluene in humin under two different levels of relative humidity. J. Environ. Qual., 31(3), 970-978 (2002).

9. Shih, Y.H. and S.C. Wu, Sorption kinetics of selected volatile organic compounds in humin. Environ. Toxicol. Chem., 21(10), 2067-2074 (2002).

10. Brusseau, M.L. and P.S.C. Rao, Sorption nonideality during organic contaminant transport in porous media. Crit. Rev. Environ. Control, 19(1), 33-39 (1989).

11. Culver, T.B., R.A. Brown and J.A. Smith, Rate-limited sorption and desorption of 1,2-dichlorobenzene to a nature sand soil column. Environ. Sci. Technol., 34(12), 2446-2452 (2000).

12. Johnson, G.R., K. Gupta, D.K. Putz, Q. Hu and M.L. Brusseau, The effect of local-scale physical heterogeneity and nonlinear, rate-limited sorption/desorption on contaminant transport in porous media. J. Contam. Hydrol., 64(1-2), 35-58 (2003).

13. Johnson, G.R., Z. Zhang and M.L. Brusseau, Characterizing and quantifying the impact of immiscible-liquid dissolution and nonlinear, rate-limited sorption/desorption on low-concentration elution tailing. Water Resour. Res., 39(5), 1120-1127 (2003).

14. Maraqa, M. A., Prediction of mass-transfer coefficient for solute transport in porous media. J. Contam. Hydrol., 53(1-2), 153-171 (2001).

15. Pang, L. and M. Close, Field-scale physical non-equilibrium transport in an alluvial gravel aquifer. J. Contam. Hydrol., 38(4), 447-464 (1999).

16. Rabideau, A.J. and C.T. Miller, Two-dimensional modeling of aquifer remediation influenced by sorption nonequilibrium and hydraulic conductivity heterogeneity. Water Resour. Res., 30(5), 1457-1470 (1994).

17. Seyfried, M.S. and P.S.C. Rao, Solute transport in undisturbed columns of an aggregated tropical soil: Preferential flow effects. Soil Sci. Soc. Am. J., 51(6), 1434-1444 (1987).

18. van Genuchten, M.T. and P.J. Wierenga, Mass transfer studies in sorbing porous media: II. Experimental evaluation with tritium (^3H_2O). Soil Sci. Soc. Am. J., 41(2), 272-278 (1977).

19. Zhang, Z. and M.L. Brusseau, Nonideal transport of reactive solutes in heterogeneous porous media 5. Simulating regional-scale behavior of a trichloroethene plume during pump-and-treat remediation. Water Resour. Res., 35(10), 2921-2935 (1999).

20. Culver, T.B., S.P. Hallisey, D. Sahoo, J.J. Deitsch and J.A. Smith, Modeling the desorption of organic contaminants from long-term contaminated soil using distributed mass transfer rates. Environ. Sci. Technol., 31(6), 1581-1588 (1997).

21. Deitsch , J.J., J.A. Smith, T.B. Culver, R.A. Brown and S.A. Riddle, Distributed-rate model analysis of 1,2-dichlorobenzene batch sorption and desorption rates for five natural sorbents. Environ. Sci. Technol., 34(8), 1469-1476 (2000).

22. Wang, M.S., S.C. Wu, W.J. Chen and H.L. Hsu, Modeling non-equilibrium solute transport in heterogeneous soils with consideration of mass-transfer processes and the effects of vadose zone properties. Environ. Eng. Sci., 24(4), 535-549 (2007).

23. Wu, S.C. and P.M. Gschwend, Sorption kinetics of

hydrophobic organic compounds to natural sediments and soils. Environ. Sci. Technol., 20(8), 717-725 (1986).

24. Buchan, G.D., Applicability of the simple lognormal model to particle-size distribution in soils. Soil Sci., 147(3), 155-161 (1989).

25. Buchan, G.D., K.S. Grewal and A.B. Robson, Improved models of particle-size distribution: An illustration of model comparison techniques. Soil Sci. Soc. Am. J., 57(4), 901-908 (1993).

26. Shirazi, M.A., L. Boersma and J.W. Hart, A unifying quantitative analysis of soil texture: Improvement of precision and extension of scale. Soil Sci. Soc. Am. J., 52(1), 181-190 (1988).

27. Haggerty, R. and S.M. Gorelick, Modeling mass transfer processes in soil columns with pore-scale heterogeneity. Soil Sci. Soc. Am. J., 62(1), 62-74 (1998).

28. Pedit, J.A. and C.T. Miller, Heterogeneous sorption processes in subsurface systems. 1. Model formulations and applications. Environ. Sci. Technol., 28(12), 2094-2104 (1994).

29. Page, A.L., R.H. Miller and D.R. Keeney, Eds., Methods of Soil Analysis. Crop Science Society of America (CSSA) and Soil Science Society of America (SSSA), USA (1982).

30. Ott, W.R., Environmental Statistics and Data Analysis. Lewis Publisher, Boca Raton, FL (1994).

31. Chiou, C.T. and T.D. Shoup, Soil sorption of organic vapors and effects of humidity on sorptive mechanism and capacity. Environ. Sci. Technol., 19(12), 1196-1200 (1985).

32. Freeze, R.A. and J.A. Cherry, Groundwater. Prentice-Hall, Inc., Englewood Cliffs, NJ (1979).

33. Crank, J., The Mathematics of Diffusion. Oxford, Clarendon Press, London, UK (1975).

34. Schwarzenbach, R.P., P.M. Gschwend and D.M. Imboden, Environmental Organic Chemistry. John Wiley & Sons, Inc., Hoboken, NJ (2003).